Polo-like kinase 1 selective inhibitor BI2536 (dihydropteridinone) disrupts centrosome homeostasis via ATM-ERK cascade in adrenocortical carcinoma

RUEI-CI LIN[1,2*], YU-YING CHAO[2*], WEI-CHIH LIEN[3], HUEI-CIH CHANG[3], SHIH-WEI TSAI[4] and CHIA-YIH WANG[1,2]

[1]Department of Cell Biology and Anatomy, College of Medicine, National Cheng Kung University, Tainan 701; [2]Institute of Basic Medical Sciences, College of Medicine, National Cheng Kung University; [3]Department of Physical Medicine and Rehabilitation, National Cheng Kung University Hospital, College of Medicine, National Cheng Kung University; [4]Department of Obstetrics and Gynecology, An Nan Hospital, China Medical University, Tainan 709, Taiwan, R.O.C.

Received March 15, 2023; Accepted July 7, 2023

DOI: 10.3892/or.2023.8604

Abstract. Adrenocortical carcinoma (ACC) is a rare but malignant tumor. Surgical removal, radiotherapy and combined chemotherapy are commonly used to treat ACC. Despite efforts for several decades, the mortality rate of ACC remains high after treatments. Therefore, identifying a novel therapeutic molecule is important to increase the survival rate of patients with ACC. The centrosome is a microtubule organizing center, and it also functions as a signaling hub to coordinate cell cycle progression. Deficiencies in the regulation of centrosome copy numbers may cause cell cycle arrest or even apoptosis. BI2536 is a polo like kinase 1-selective inhibitor and has been tested for the treatment of several types of cancer, including lung, oral and gastric cancer. However, to the best of our knowledge, its effects on ACC have not yet been examined. The present study revealed that BI2536 inhibited Y1 ACC cell proliferation in a time- and dose-dependent manner. BI2536 blocked cell cycle progression and also induced cell apoptosis as shown by flow cytometry. Furthermore, following BI2536 treatment, centrosome amplification was induced, which resulted in aberrant mitosis. In terms of the mechanism, BI2536 induced DNA damage as evidenced by γH2AX staining and comet assay, followed by activation of ATM serine/threonine kinase-ERK signaling to promote centrosome amplification. Therefore, the present study suggested that BI2536 could be used as an adjuvant therapy in the treatment of ACC, and also revealed the underlying molecular mechanism.

Correspondence to: Professor Chia-Yih Wang, Department of Cell Biology and Anatomy, College of Medicine, National Cheng Kung University, 1 University Road, East, Tainan 701, Taiwan, R.O.C.
E-mail: b89609046@gmail.com

Dr Shih-Wei Tsai, Department of Obstetrics and Gynecology, An Nan Hospital, China Medical University, Section 2, 66 Changhe Road, Annan, Tainan 709, Taiwan, R.O.C.
E-mail: shiweitw@me.com

*Contributed equally

Key words: adrenocortical carcinoma, BI2536, centrosome, ATM serine/threonine kinase, ERK

Introduction

Adrenocortical carcinoma (ACC) is a rare malignancy with an incidence of 1-2 per million individuals per year (1). ACC is associated with poor outcomes due to overproduction of hormones (2). Hypercortisolism is often observed in patients with ACC. High cortisol levels lead to plethora, diabetes mellitus, sarcopenia, and osteoporosis. Additionally, excessive cortisol induces glucocorticoid-mediated mineralocorticoid receptor activation. Thus, hypokalemia and hypertension are also observed in ACC. High adrenal androgen levels are also observed in ACC, leading to rapid-onset male pattern baldness, virilization and menstrual irregularities in women (3). Excessive hormones are often recognized late in clinical settings, which impedes diagnosis and treatment.

Due to the complexity and poor prognosis of ACC, surgery, radiotherapy and chemotherapies, including etoposide, doxorubicin, cisplatin and mitotane, are mainly used to treat ACC (4). Despite a number of efforts to develop novel therapeutic strategies, it appears that using current agents is not sufficient to increase the therapeutic responses. Trials developing novel targeted molecules may be promising (5).

BI2536 is a polo like kinase 1 (PLK1)-selective inhibitor. At low concentrations (within the nanomolar range), it binds to the ATP-binding domain of PLK1 to inhibit the kinase activity (6). BI2536 treatment induces apoptosis by activating caspase-3 or caspase-8 in human cancer cell lines of diverse tissue origins (7,8). Notably, the antitumor effects of BI2536 have further been demonstrated using human tumor xenografts in nude mouse models. Thus, BI2536 has been

studied in clinical studies in patients with locally advanced or metastatic cancer.

The centrosome is the major microtubule organizing center of mammalian cells. By recruiting γ-tubulin ring complexes to the pericentriolar materials of the centrosome, the centrosome nucleates microtubules from the minus-end to the plus-end to orchestrate the microtubule arrays (9). In addition to organizing the microtubules, the centrosome also regulates cell cycle progression during interphase and orchestrates mitotic spindle formation at M phase (10). Thus, deficiencies in centrosome structure or function may impede cell cycle progression or even trigger apoptotic cell death (11). Normally, each cell contains one centrosome. Coordinated with DNA replication, the centrosome starts to duplicate at S phase through CDK2 activation. At G_2/M transition, the duplicated centrosomes become mitotic spindle poles and separate to the opposite of the nucleus to align and segregate the replicated chromosomes into each daughter cell. Thus, precise control of centrosome homeostasis is important to maintain genome integrity.

BI2536 has been tested for the treatment of several cancer types, including oral, lung and gastric cancer (12-14); however, to the best of our knowledge, its effects on adrenocortical tumors have not been tested yet. The present study revealed that BI2536 inhibited Y1 adrenocortical cell proliferation by blocking cell cycle progression and inducing apoptosis. Mechanistically, BI2536 induced centrosome amplification and aberrant mitotic spindle poles by activating the ATM serine/threonine kinase (ATM)-ERK cascade. Therefore, the present study demonstrated that BI2536 could potentially be used for the treatment of adrenocortical tumors, and the underlying molecular mechanism was also revealed.

Materials and methods

Cell culture. The Y1 mouse adrenocortical tumor, H295R human adrenocortical tumor and NIH3T3 mouse embryonic fibroblast cell lines were cultured in DMEM-F12 full medium containing 10% FBS in a humidified atmosphere with 5% CO_2 at 37˚C. Y1, H295R cell lines and NIH3T3 were kindly provided by Dr Bon-chu Chung (Academia Sinica, Taipei, Taiwan). Mycoplasma contamination was regularly checked by DAPI staining.

The following drugs were used in the present experiments: Vanillin [DNA-dependent protein kinase (DNA-PK) inhibitor; cat. no. V110-4; 1 mM, (15)], Ku55933 [competitive ATM kinase inhibitor; cat. no. SML1109; 10 μM, (16)] and U0126 [ERK inhibitor; cat. no. U120; 20 μM, (17)], which were purchased from MilliporeSigma. BI2536 (PKL1 inhibitor; cat. no. S1109; 500 nM) was purchased from Selleck Chemicals. For the drug treatments, the indicated time points are shown in the figure legends.

Cell cycle analysis. The cell cycle profiles (10^6 cells) were analyzed by FACS according to a previously described methodology (18). After treating Y1 cells with BI2536 at 500 nM for 24 h, cells were suspended in PBS containing 1 mM EDTA (PBS-E) buffer. Following centrifugation (1,000 x g for 5 min, 4˚C), the supernatant was removed, and the pellets were suspended with PBS-E buffer. Subsequently, the suspension was further centrifuged at 1,000 x g for 5 min at 4˚C, followed by removal of the supernatant. The centrifuged cells were suspended with 0.5 ml PBS-E buffer, followed by fixation of cells with 70% ethanol at 4˚C overnight. Before cell cycle analysis, ethanol was removed by centrifugation, and cells were washed with 10 ml PBS-E at least three times. Subsequently, cells were stained with propidium iodide (SouthernBiotech) for 1 h at room temperature. The cell cycle profiles were determined and analyzed using a FACScan flow cytometer (BD Biosciences) and Kaluza software Version 1.5 (Beckman Coulter, Inc.).

5-ethynyl-2'-deoxyuridine (EdU) incorporation assay. The EdU incorporation assay was performed according to the manufacturer's instructions (Invitrogen; Thermo Fisher Scientific, Inc.) and modified according to the previously described methodology (19). In brief, the drug-treated cells ($5x10^5$) were incubated with EdU for at least 8 h at 37˚C. Subsequently, the cells were washed with PBS at least three times and fixed with fixation buffer provided in the commercial kit. To count the EdU-positive cells, the fixed cells were stained with DAPI (0.5 μg/ml) in PBS at 37˚C for 10 min, and then observed using a fluorescence microscope.

Microtubule nucleation assay. To examine microtubule nucleation, cells were treated with 25 μM nocodazole in the culture medium to depolymerize the microtubules. At 1 h after microtubule depolymerization, the depolymerized cells were washed with PBS three times and then cultured in drug-free medium for the indicated time points. To observe the microtubules, the cells were fixed with ice-cold methanol, followed by staining with antibody against α-tubulin for further observation.

Comet assay. The comet assay was performed according to the manufacturer's instructions (cat. no. ab238544; Abcam). Briefly, the comet agarose (1%) was loaded onto the comet slide to form a base layer. Then, the cells were mixed with comet agarose and the mixture was loaded onto the top of the base layer. The cells were treated with the commercial lysis buffer (2.5 M NaCl, 0.1M EDTA and 10 mM Tris-HCl) and alkaline solution (1% NaOH and 1% 0.5M EDTA), followed by performing the electrophoresis under alkaline conditions. The comet tail was observed by staining with DAPI (0.5 μg/ml) at 37˚C.

Immunofluorescence microscopy. Y1 cells (10^5) were plated on coverslips overnight, followed by treatment of cells with drugs. Subsequently, the cells were washed with PBS three times and fixed with -20˚C methanol for 6 min. These cells were blocked with 1% normal goat serum for 1 h at 37˚C, followed by incubation with primary antibodies [anti-α-tubulin and anti-γ-Tubulin, GTU-88 (both at 1:700 dilution in 1% normal goat serum); and anti-γ-H2AX (phosphorylation at S139, EP854(2)Y; 1:700 dilution in 1% normal goat serum; cat. no. ab81299; Abcam)] at 4˚C overnight. Subsequently, the cells were washed with PBS with Triton X-100 (PBS-T) three times, followed by incubation with FITC (1:700; cat. no. F-2761)- or Cy3 (1:700; cat. no. A10521)-conjugated secondary antibodies (both from Invitrogen; Thermo Fisher Scientific, Inc.) at 4˚C for 1 h. Meanwhile, the nuclei were also co-stained with DAPI (0.5 μg/ml) at 37˚C for 1 h. Next, the cells were

washed again with PBS-T three times and then mounted with 50% glycerol/PBS-T on microscope slides. The fluorescence signals were examined using an AxioImager M2 fluorescence microscope (Zeiss AG).

Western blotting. Y1, H295R and NIH3T3 cell extracts were collected by lysing cells with a lysis buffer containing 0.5% NP-40, 300 mM NaCl, 1 mM EDTA and a protease inhibitor cocktail (Roche Diagnostics GmbH). After centrifugation at 15,000 x g at 4˚C, the supernatants were collected and quantified using the Bradford protein assay kit according to the instruction. Subsequently, equal amounts of extract (50 μg) were loaded per lane. 12% SDS-PAGE gels were used to separate the samples. After separation, samples were transferred to the polyvinylidene difluoride (PVDF) membranes. Membranes were blocked with 5% skim milk at room temperature for 1 h then incubated with primary antibodies (see below) at 4˚C for 12 h. Subsequently, the antibodies were washed out with TBST (TBS with 01% Tween-20) for three times and membranes were incubated with HRP-conjugated secondary antibodies at room temperature for 1 h. Finally, after washed by TBST for three times, the protein signal on membrane were detected by enhanced chemiluminescent (ECL) kit (cat. no. A38556; Thermo Fisher Scientific, Inc.).

For western blotting, the primary antibodies (1:2,000 dilution) were incubated at 4˚C for 12 h and obtained commercially: Anti-Ku70 (N3H10; cat. no. GTX23114), anti-ATM (2C1; cat. no. GTX7010), anti-ATR serine/threonine kinase (ATR; cat. no. GTX128146), anti-β-actin (AC-15; cat. no. GTX26276), anti-catalytic subunit of DNA-PK (phosphor-Thr2609; cat. no. GTX24194), anti-Akt (phosphor-Ser473; cat. no. GTX128414) and anti-p53 (DO1; cat. no. GTX70214) were purchased from GeneTex, Inc. Anti-acetylated-tubulin (cat. no. T6793) and anti-α-tubulin (cat. no. T6557) were purchased from MilliporeSigma. Anti-ATM (phosphor-Ser1981; cat. no. ab81292) was purchased from Abcam. Anti-ATR (phosphor-Ser428; cat. no. 2853), anti-checkpoint kinase 2 (Chk2; phosphor-Thr68; cat. no. 2661), anti-Chk2 (cat. no. 3440), anti-Akt (phosphor-Ser473; cat. no. 4060), anti-Akt (cat. no. 4691), anti-p44/42 MAPK (Erk1/2; phosphor-Thr202/Tyr204; cat. no. 4370), anti-p44/42 MAPK (Erk1/2; cat. no. 4695), anti-p53 (phosphor-Ser15; cat. no. 9284), anti-checkpoint kinase 1 (Chk1; phosphor-Ser317; cat. no. 12302) and anti-Chk1 (cat. no. 2360) were purchased from Cell Signaling Technology, Inc. Anti-p150^{glued} (cat. no. 610473) was purchased from BD Biosciences. Goat anti-rabbit (1:7,000; cat. no. 31460) or anti-mouse (1:7,000; cat. no. 31430) IgG (H+L), HRP-conjugated secondary antibodies (Invitrogen; Thermo Fisher Scientific, Inc.) were incubated at 37˚C for 1 h.

Mitotic index. The proportions of mitotic cells were identified and quantified according to a previously described protocol (9). In brief, according to the chromosome alignments, the mitotic cells at different phases of M phase were quantified. In each independent experiment, >1,000 cells were counted using an AxioImager M2 fluorescence microscope (Carl Zeiss AG).

Statistical analysis. The mean ± SD of three independent experiments is presented for all data. In each individual group, ≥100 cells were counted. Differences between two individual experiments were compared using two-tailed Student's t-tests (unpaired) or one-way ANOVA. Tukey's multiple comparison test was performed as a post hoc test. $P<0.05$ was considered to indicate a statistically significant difference.

Results

BI2536 inhibits ACC cell growth. BI2536 has been used to treat several cancer types; however, to the best of our knowledge, its effect on adrenocortical tumors has not yet been examined. In the present study, it was for the first time analyzed whether BI2536 inhibited the proliferation of Y1 mouse adrenocortical cancer cells. BI2536 inhibited Y1 cell proliferation in a dose-dependent manner (Fig. 1A), and the IC_{50} of BI2536 in Y1 cells was ~500 nM, thus this concentration was used in the following experiments. Subsequently, Y1 cells were treated with 500 nM BI2536 for 24, 48 and 72 h, and it was revealed that BI2536 inhibited Y1 cell proliferation in a time-dependent manner (Fig. 1B). Since mitotane is used to treat adrenocortical tumors in clinical practice, the present study examined the IC_{50} of mitotane on Y1 cell proliferation. After treating Y1 cells with mitotane at different concentrations for 24 h, it was demonstrated that the IC_{50} of mitotane on Y1 cell proliferation was ~25 μM (Fig. 1C), which was 50-fold higher than that of BI2536. The data suggested that BI2536 could be a good candidate small compound for the treatment of adrenocortical tumors. The present study also examined the effects of BI2536 on the H295R human adrenocortical cancer cell line. At a concentration of 500 nM, BI2536 inhibited H295R cell proliferation (Fig. 1D). The cytotoxic effect of BI2536 on normal cells was also examined. Treatment of NIH3T3 cells (mouse embryonic fibroblast cells) with 500 nM BI2536 had no effect on NIH3T3 cell proliferation (Fig. 1E). Thus, BI2536 reduced adrenocortical tumor cell proliferation.

The cell cycle profiles were subsequently analyzed by flow cytometry. Following 500 nM BI2536 treatment for 24 h, the proportions of Y1 cells at sub-G_1 phase were significantly increased, while those at G_0/G_1 and S phase were reduced (Fig. 2A and B). Subsequently, the ability of cells to enter into S phases was examined using an EdU incorporation assay. The proportions of EdU-positive cells were significantly reduced in BI2536-treated cells (Fig. 2C and D). In addition, the mitotic index in BI2536-treated Y1 cells was reduced, suggesting that BI2536 also inhibited entry of cells into M phase (Fig. 2E). Thus, BI2536 induced apoptosis and impeded cell cycle progression.

When examining nuclear staining, aberrant nuclear shapes, including mostly di-nuclei, micro-nuclei and enlarged nuclei, were observed in BI2536-treated cells, suggesting that genomic instability occurred (Fig. 3A-D). Genomic instability may be caused by aberrant mitosis, thus the mitotic spindle poles in the absence or presence of BI2536 were examined. Normally, two mitotic spindle poles (as shown by γ-tubulin staining) located at the opposite sites of the cell to align the duplicated chromosomes at the equatorial plate (Fig. 4A, left panel). However, when the cells were treated with BI2536, aberrant mitotic spindle poles were observed (Fig. 4A, right panel, and B), and the chromosomes were not aligned well during mitosis. Thus, BI2536 induced aberrant mitosis.

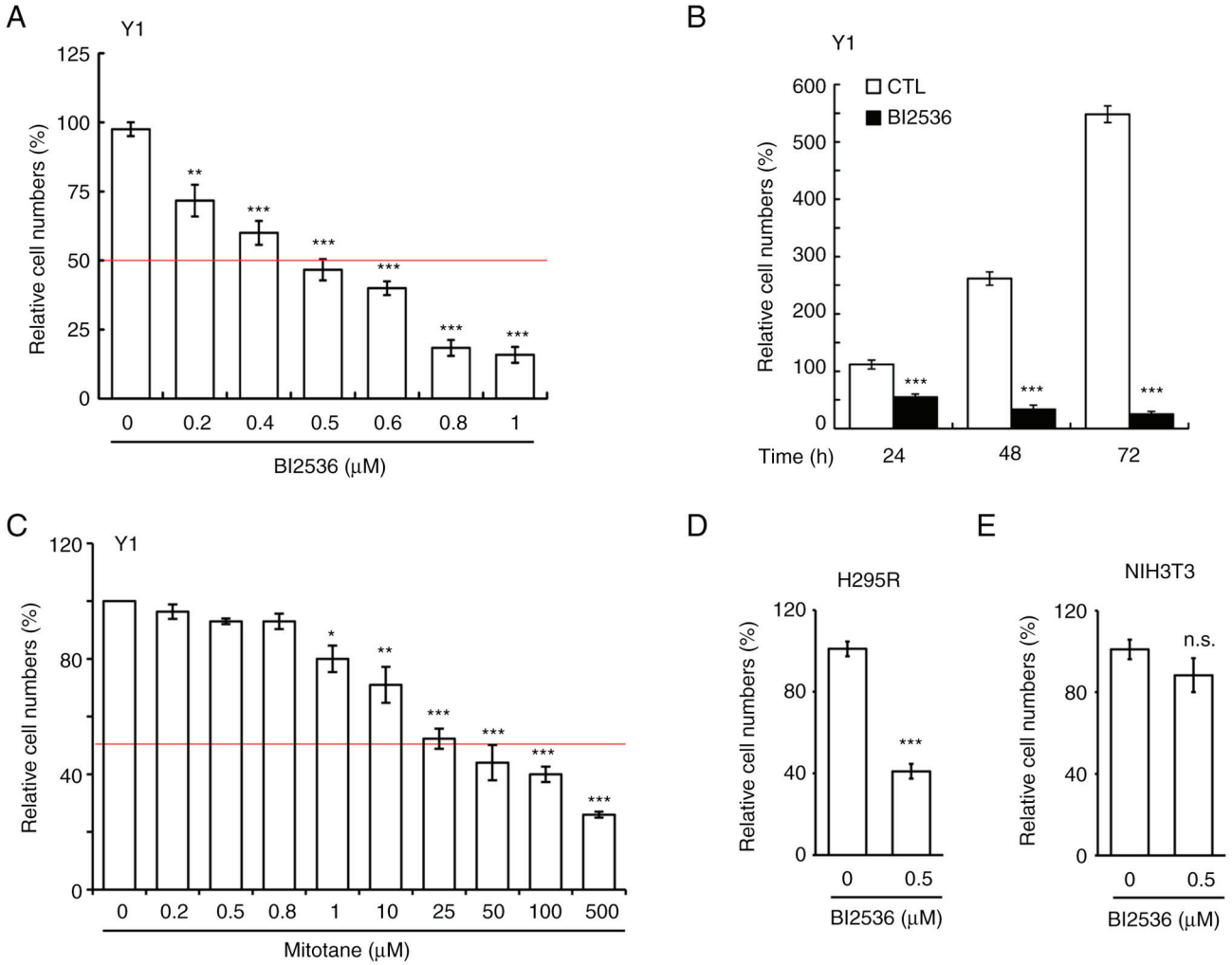

Figure 1. BI2536 inhibits ACC cell proliferation. (A) ACC cell proliferation assay. The IC_{50} of BI2536 was 500 nM. Y1 cells were treated with different concentrations of BI2536, followed by counting of cell numbers. The red line indicates the IC_{50} of BI2536. (B) BI2536 inhibits ACC cell proliferation in a time-dependent manner. Y1 cells were treated with 500 nM BI2536 for 24, 48 or72 h. (C) ACC cell proliferation assay. The IC_{50} of mitotane was 25 μM. Y1 cells were treated with different concentrations of mitotane, followed by counting of cell numbers. The red line indicates the IC_{50} of mitotane. (D) BI2536 inhibits H295R cell proliferation. H295R cells were treated with 500 nM BI2536 for 24 h, followed by counting of cell numbers. (E) BI2536 did not affect NIH3T3 cell proliferation. NIH3T3 cells were treated with 500 nM BI2536 for 24 h, followed by counting of cell numbers. These results are presented as the mean ± SD of three independent experiments. *P<0.05, **P<0.01 and ***P<0.001. ACC, adrenocortical carcinoma; CTL, vehicle control; n.s., no significance.

BI2536 induces centrosome amplification. Mitotic spindle poles were caused by centrosome amplification (cells with ≥3 centrosomes) (20). The centrosome copy numbers during interphase were subsequently examined. Normally, cells contained one (before duplication) or two (after duplication) centrosomes; however, following BI2536 treatment, centrosome amplification was observed in both Y1 and H295R cells (Figs. 4C and D, and S1A), suggesting that BI2536 disrupted centrosome homeostasis. The centrosome is the microtubule organizing center, and the present study subsequently investigated whether these amplified centrosomes were functional. The microtubules were depolymerized by treating cells with nocodazole for 1 h, followed by washing out the drugs to regrow the microtubules. After depolymerization, the microtubules were not observed in the control cells. However, 1 min after drug washout, the microtubules started to nucleate, and after 10 min, microtubule arrays were established in the cytoplasm (Fig. 4E, upper panel). The ability of the microtubules to regrow in BI2536-treated cells was similar to that in the control cells (Fig. 4E, lower panel). Thus, BI2536 induced centrosome amplification without affecting microtubule nucleation.

BI2536 induces centrosome amplification by activating ATM. DNA damage induces centrosome amplification (15), thus the present study investigated whether BI2536 facilitated centrosome amplification through DNA damage. First, it was examined whether BI2536 induced DNA damage. The DNA damage marker γ-H2AX was examined using immunofluorescence staining. Following BI2536 treatment, the proportion of γ-H2AX-positive cells was markedly increased (Fig. 5A), suggesting that BI2536 induced DNA damage. To further confirm the present finding, a comet assay was performed. In the presence of DNA damage, a comet tail was formed (Fig. 5B). Following BI2536 treatment, the proportion of comet tail-positive samples was increased, indicating that BI2536 induced DNA damage (Fig. 5C). Next, it was examined whether the DNA damage response induced centrosome amplification. The phosphoinositide 3 kinase-related protein

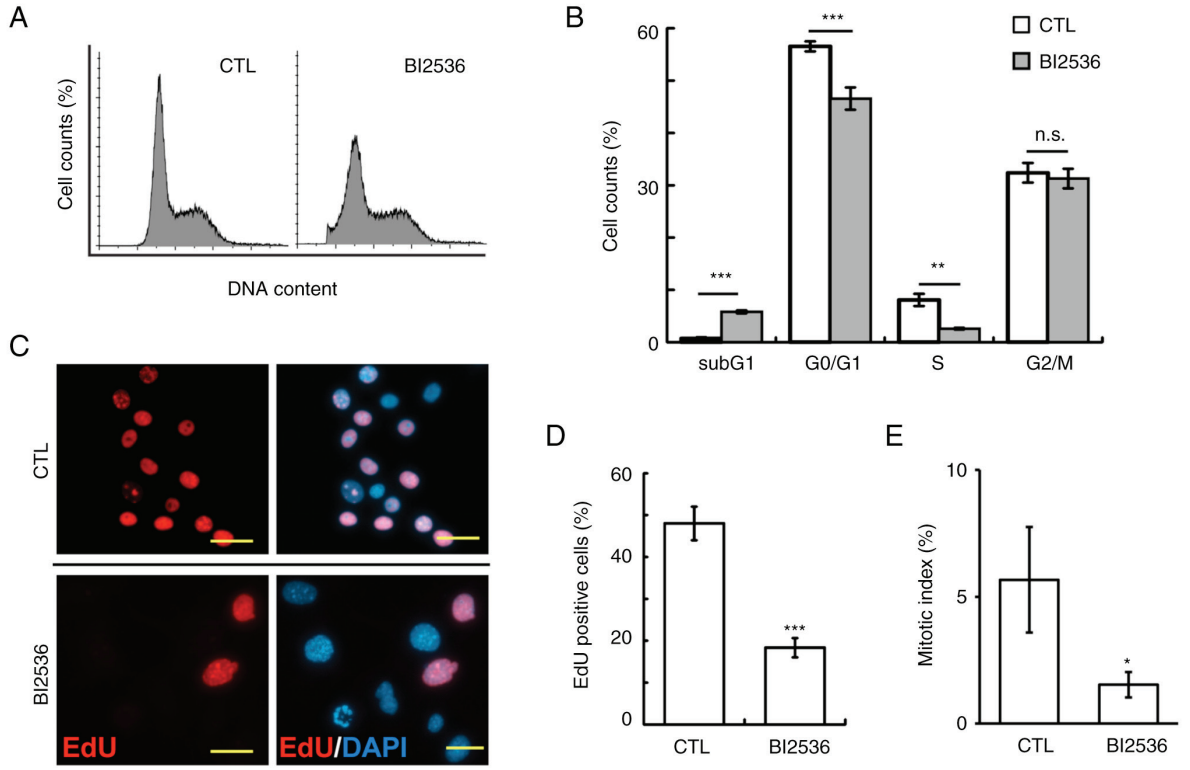

Figure 2. BI2536 inhibits cell cycle progression. (A and B) BI2536 induced apoptosis and reduced the proportion of cells in G_0/G_1 and S phases. (A) Cell cycle progression of BI2536-treated Y1 cells was analyzed by flow cytometry. (B) Quantification of Y1 cells in different cell cycle stages in the presence or absence of BI2536. (C and D) EdU incorporation was reduced in BI2536-treated Y1 cells. (C) Immunostaining with EdU (red) and DAPI (blue) in CTL or BI2536-treated Y1 cells. Scale bar, 20 μm. (D) Quantification of EdU-positive CTL or BI2536-treated Y1 cells. (E) BI2536 inhibited mitosis of Y1 cells. Quantification of mitotic index of CTL or BI2536-treated Y1 cells. These results are presented as the mean ± SD of three independent experiments; >1,000 cells were counted in each individual group. *P<0.05, **P<0.01 and ***P<0.001. CTL, scramble control; EdU, 5-ethynyl-2'-deoxyuridine; n.s., no significance.

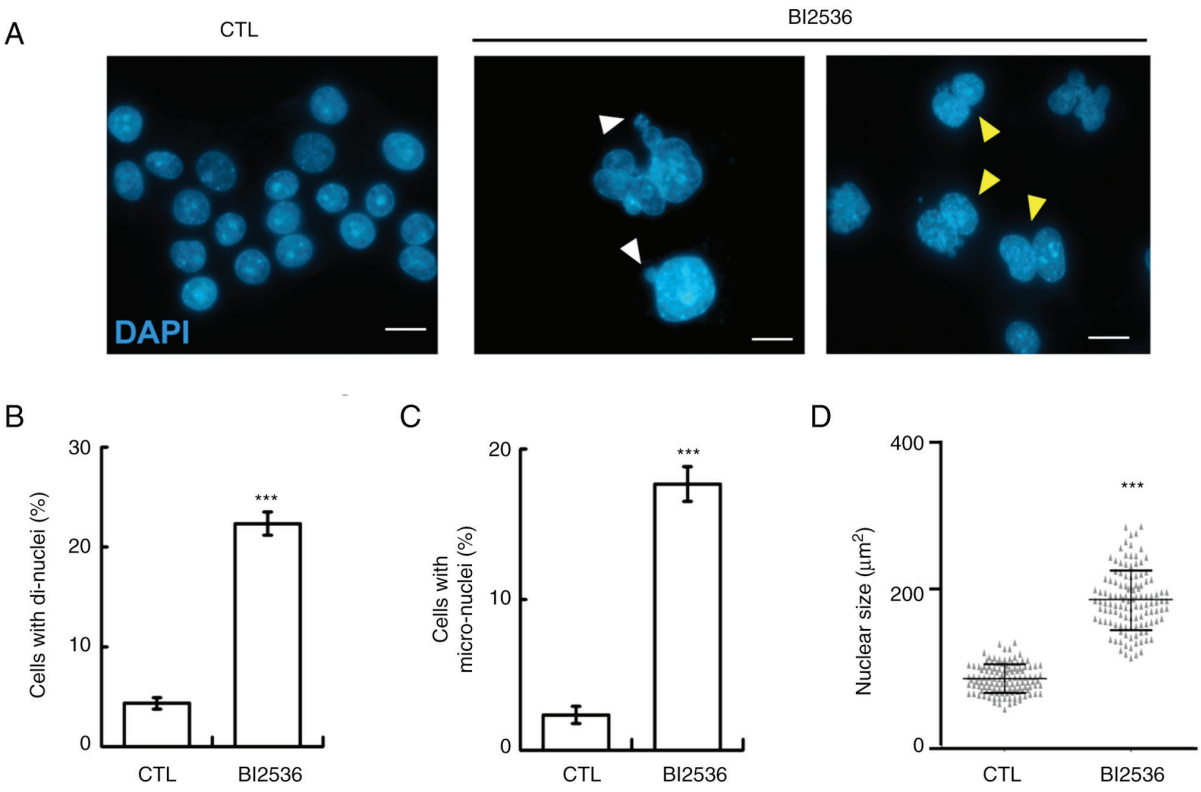

Figure 3. Genomic instability is observed in BI2536-treated Y1 cells. (A) Immunostaining of cells with DAPI to observe the morphologies of nuclei. White arrowhead, micro-nuclei; yellow arrowhead, di-nuclei. Scale bar, 10 μm. (B-D) Quantifications of cells with (B) di-nuclei, (C) micro-nuclei or (D) enlarged nuclei in the absence (CTL) or presence of BI2536. The results are presented as the mean ± SD of three independent experiments; >1,000 cells were counted in each individual group. ***P<0.001. CTL, control; n.s., no significance.

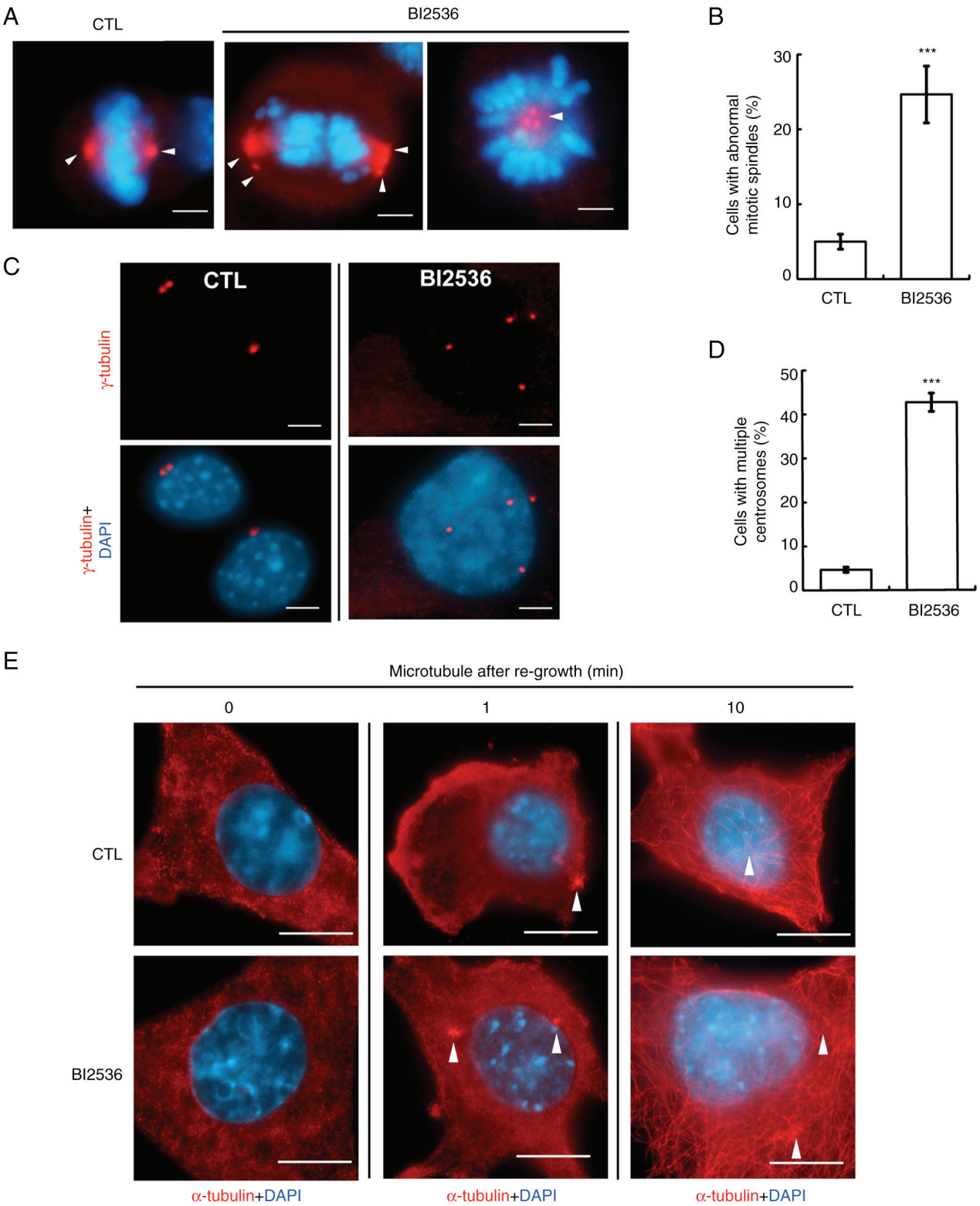

Figure 4. BI2536 induces centrosome amplification. (A and B) BI2536 induced aberrant mitotic spindle poles. (A) Mitotic spindle poles (arrowhead) were observed by immunostaining with an antibody against γ-tubulin. Nuclei were shown by DAPI staining. (B) Quantification results for (A). (C and D) Centrosome amplification (≥2 centrosomes) was observed by immunostaining with an antibody against γ-tubulin. Nuclei were shown by DAPI staining. (D) Quantification results for (C). (E) Microtubule nucleation activity was examined by disrupting microtubules (0 min), followed by regrowing the microtubules for 1 or 10 min in the presence or absence of BI2536. Microtubules were stained with α-tubulin. DNA was stained with DAPI. Scale bar, (A and C) 5 μm or (E) 10 μm. The results are presented as the mean ± SD of three independent experiments; >100 cells were counted in each individual group. ***P<0.001. CTL, control.

kinases, including ATM, ATR and DNA-PK, were examined. ATM and DNA-PK, but not ATR, were activated by BI2536 treatment (Figs. 5D and E, and S1B). Subsequently, the effects of these two kinases on centrosome amplification were examined. Ku55933 inhibited the activation of ATM (Fig. 5F) and centrosome amplification (Fig. 5G). However, inhibition

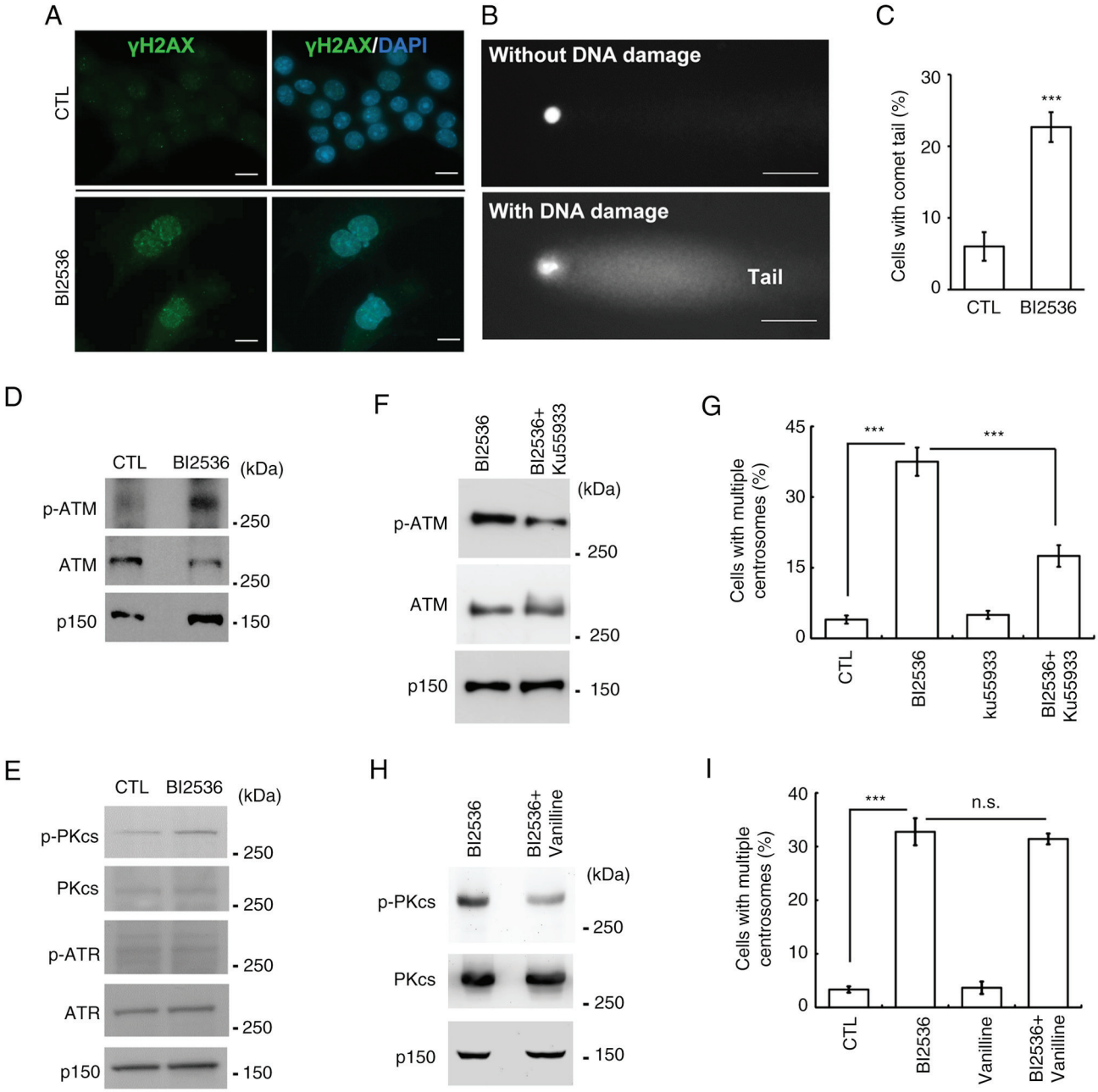

Figure 5. ATM contributes to centrosome amplification following BI2536 treatment. (A-C) DNA damage was induced in BI2536-treated Y1 cells. DNA damage was detected by immunostaining with an antibody against γ-H2AX. DNA was shown by DAPI staining. Scale bar, 10 μm. (B) DNA damage was examined using a comet assay. Representative images of cells without (upper panel) or with (lower panel) DNA damage. Scale bar, 10 μm. (C) Quantitative results for (B). (D and E) ATM and DNA-PK were activated by BI2536 treatment. Cell extracts of CTL or BI2536-treated cells were analyzed by western blotting with antibodies against ATM, p-ATM, ATR, p-ATR, DNA-PKcs and p-DNA-PKcs. P150 was used as a loading control. (F-I) Inhibition of (F and G) ATM but not (H and I) DNA-PK alleviated BI2536-induced centrosome amplification. (F and H) ATM and DNA-PK were inhibited by (F) Ku55933 and (H) vanillin, respectively. Quantitative results of cells with centrosome amplification in the presence or absence of (G) ATM inhibitor (Ku55933) or (I) DNA-PK inhibitor (vanillin). ***P<0.001. ATM, ATM serine/threonine kinase; ATR, ATR serine/threonine kinase; CTL, control; DNA-PK, DNA-dependent protein kinase; DNA-PKcs, catalytic subunit of DNA-PK; n.s., no significance; p-, phosphorylated; P150, p150^{glued}.

of DNA-PK by treating cells with vanillin had no effect on centrosome amplification (Fig. 5H and I). Thus, BI2536 induced centrosome amplification by activating ATM.

BI2536 activates the ATM-ERK axis to induce centrosome amplification. The downstream effectors of the DNA damage response were next examined. Canonical effectors, including Akt, Chk1 and Chk2, were not activated by BI2536 (Fig. 6A). ERK activation induces centrosome amplification (3). The present study then examined whether ERK participated in BI2536-induced centrosome amplification. Following BI2536 treatment, ERK was activated in a dose-dependent manner (Figs. 6B and S1C). Treatment with U0126, an ERK-selective inhibitor, inhibited ERK activation and alleviated BI2536-induced centrosome amplification (Fig. 6C and D). The data suggested that BI2536 activated ERK to induce centrosome amplification. The present study then examined whether ERK was activated by ATM. Inhibition of ATM

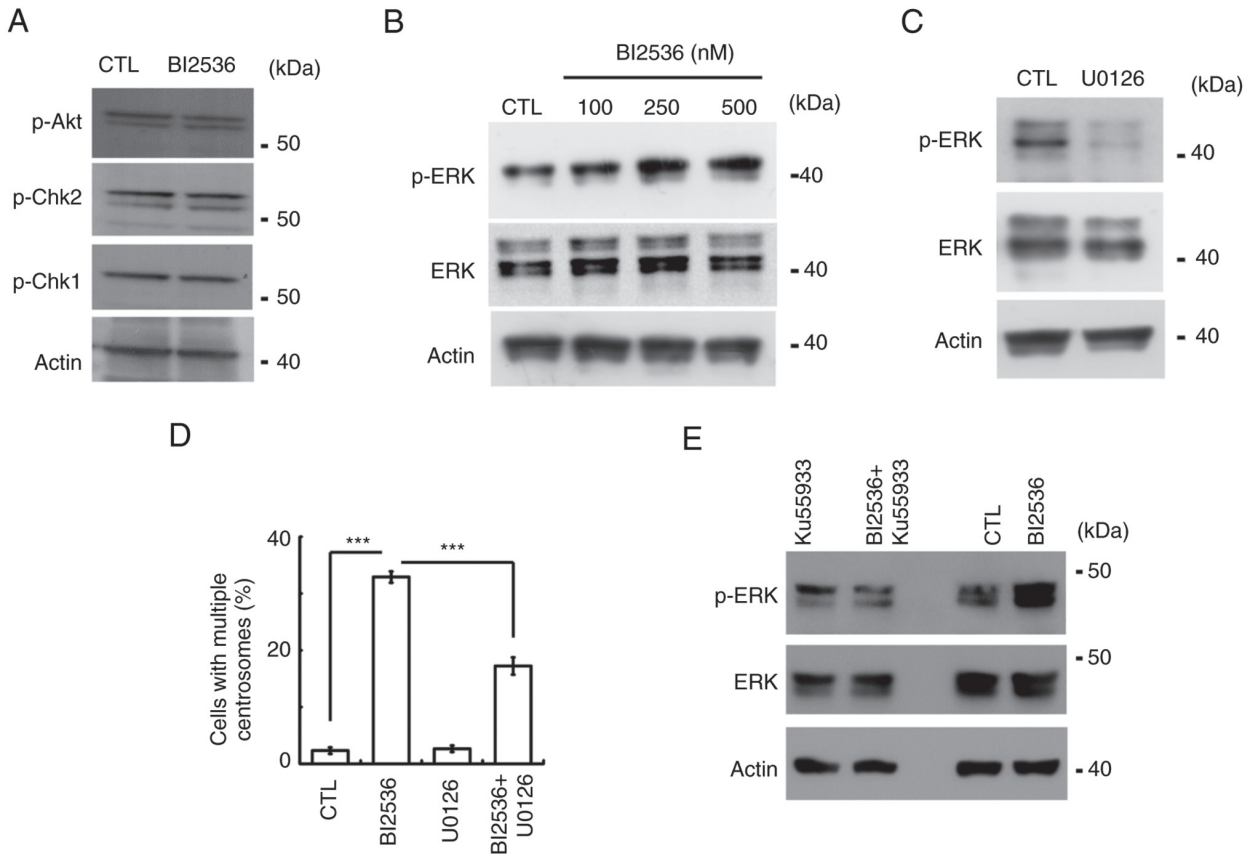

Figure 6. ERK activation participates in BI2536-induced centrosome amplification. (A) BI2536 did not activate effector kinases. Extracts of CTL or BI2536-treated cells were analyzed by western blotting with antibodies against p-Akt, p-Chk1, p-Chk2 or actin. (B) ERK was dose-dependently activated by BI2536. Extracts of CTL or BI2536-treated cells were analyzed by western blotting with antibodies against p-ERK, ERK or actin. (C) Activation of ERK was inhibited by U0126 (ERK selective inhibitor). Extracts of CTL or U0126-treated cells were analyzed by western blotting with antibodies against p-ERK, ERK or actin. (D) Inhibition of ERK alleviated BI2536-induced centrosome amplification. Quantitative results of cells with centrosome amplification in the absence or presence of ERK inhibitor (U0126). (E) Inhibition of ATM serine/threonine kinase reduced ERK activation in the presence of BI2536. Extracts of CTL or U0126-treated cells were analyzed by western blotting with antibodies against p-ERK, ERK or actin. Chk1, checkpoint kinase 1; Chk2, checkpoint kinase 2; ***P<0.001; CTL, control; p-, phosphorylated.

reduced ERK activation in both Y1 and H295R cells (Figs. 6E and S1D). Thus, the present data indicated that BI2536 activated the ATM-ERK axis to induce centrosome amplification in adrenocortical tumor cells.

Discussion

The present study revealed that BI2536 inhibited cell proliferation and induced apoptosis in ACC. Following BI2536 treatment, DNA damage occurred, followed by activation of the ATM-ERK signaling cascade to induce centrosome amplification. Aberrant centrosome copy numbers impeded cell cycle progression and apoptosis, thus reducing adrenocortical tumor cell proliferation. Therefore, BI2536 could be used as an adjuvant chemotherapeutic drug for the treatment of ACC.

Mitotane, a derivative of the insecticide dichlorodiphenyltrichlorethane, is approved by the Federal Drug Administration, USA, to treat ACC in clinical practice. However, the limitation of this drug, including low efficacy and a narrow therapeutic window, and its serious toxicity prompt the authors to identify a novel adjuvant therapeutic molecule (4,5). BI2536 treatment induces apoptosis in human cancer cell lines of diverse tissue origins (7,8). Notably, the antitumor effects of BI2536 have further been demonstrated using human tumor xenografts in nude mouse models. The present study revealed that BI2536 (~500 nM) inhibited ACC cell proliferation efficiently when compared with mitotane (~25 μM). In addition, treatment of BI2536 at 500 nM did not affect the growth of fibroblast cells, suggesting its biosafety in normal cells. Moreover, BI2536 has been tested in phase II clinical trials. Thus, the present study suggested that BI2536 could be tested in clinical studies in patients with ACC or used as an adjuvant therapy to accelerate the chemotherapeutic efficiency.

The centrosome is not only a microtubule organizing center but also required for controlling cell cycle progression. For example, centrosomal targeting of cyclin E or cyclin A is required for S phase entry (21). DNA replication-related proteins, including minichromosome maintenance complex component 5 and origin recognition complex subunit 1, are also localized to the centrosome to regulate centrosome duplication (22). Thus, the crosstalk between the nucleus and centrosome appears to be an important issue in regulating cell cycle progression properly. Previous studies have demonstrated that some DNA damage-related protein also localized to the centrosome to modulate centrosome copy numbers. Both the regulatory and catalytic subunits of DNA-PK are recruited

to the centrosome and the activated centrosomal DNA-PK induces centrosome amplification (15,16). In osteosarcoma, checkpoint protein Chk2 is aberrantly increased in the centrosome, thus inducing centrosome amplification following DNA damage. The present study revealed that ATM was activated following BI2536 treatment. It is known that active ATM is mainly localized in the nucleus; however, during mitosis, active ATM is observed in the mitotic spindle poles where it is involved in the maintenance of mitosis. Thus, it was hypothesized that BI2536-activated ATM localized to both the nucleus and centrosome. In the nucleus, ATM initiated the DNA damage response; in the centrosome, it facilitated centrosome amplification. Thus, distinct subcellular compartments of ATM may perform different cellular functions.

BI2536 is a PLK1-selective inhibitor. The present study revealed that BI2536 induced DNA damage and activated DNA damage responses. Previous studies have demonstrated that, in response to high levels of replication stress or DNA damage, PLK1 phosphorylates several targeted proteins such as primase and DNA directed polymerase, RAD51 recombinase, BRCA2 and MRE11, and is implicated in the DNA damage response (23-26). However, how inhibition of PLK1 induces DNA damage under basal conditions remains less studied. PLK1 interacts with CDK1 to maintain cell cycle progression (27). CDK1 also participates in homologous recombination-dependent repair of DNA double-strand breaks, and couple DNA damage repair to cell cycle progression (28,29). The present study revealed that ATM and DNA-PK, two kinases responsible for DNA double-strand breaks, were activated when PLK1 was inhibited. Thus, it was hypothesized that, when PLK1 was inhibited, the activity of CDK1 was reduced, leading to DNA double-strand breaks. However, this hypothesis still needs to be further confirmed in the future.

Acknowledgements

The authors are grateful for the support from the Core Research Laboratory, College of Medicine, National Cheng Kung University. The authors also appreciate Dr Bon-chu Chung (Academia Sinica, Taipei, Taiwan) for kindly providing Y1 and H295R cell lines.

Funding

The present study was supported by the Ministry of Science and Technology of Taiwan (grant nos. MOST106-2320-B-006-056-MY3andMOST109-2320-B-006-042-MY3) and by An Nan Hospital, China Medical University (grant no. ANHRF111-17).

Availability of data and materials

The datasets used and/or analyzed during the current study are available from the corresponding author on reasonable request.

Authors' contributions

C-YW and S-WT conceptualized the study. R-CL, Y-YC, W-CL and H-CC implemented methodology. R-CL, Y-YC, W-CL and H-CC conducted investigation. R-CL, Y-YC, W-CL and H-CC performed software and formal analysis. S-WT and C-YW wrote, reviewed and edited the manuscript. S-WT and C-YW supervised the study and acquired funding. R-CL and C-YW confirm the authenticity of all the raw data. All authors read and approved the final version of the manuscript.

Ethics approval and consent to participate

Not applicable.

Patient consent for publication

Not applicable.

Competing interests

The authors declare that they have no competing interests.

References

1. Long SE and Miller BS: Adrenocortical cancer treatment. Surg Clin North Am 99: 759-771, 2019.
2. Abiven G, Coste J, Groussin L, Anract P, Tissier F, Legmann P, Dousset B, Bertagna X and Bertherat J: Clinical and biological features in the prognosis of adrenocortical cancer: Poor outcome of cortisol-secreting tumors in a series of 202 consecutive patients. J Clin Endocrinol Metab 91: 2650-2655, 2006.
3. Chen TY, Syu JS, Lin TC, Cheng HL, Lu FL and Wang CY: Chloroquine alleviates etoposide-induced centrosome amplification by inhibiting CDK2 in adrenocortical tumor cells. Oncogenesis 4: e180, 2015.
4. Fassnacht M, Terzolo M, Allolio B, Baudin E, Haak H, Berruti A, Welin S, Schade-Brittinger C, Lacroix A, Jarzab B, *et al*: Combination chemotherapy in advanced adrenocortical carcinoma. N Engl J Med 366: 2189-2197, 2012.
5. Libé R: Adrenocortical carcinoma (ACC): Diagnosis, prognosis, and treatment. Front Cell Dev Biol 3: 45, 2015.
6. Steegmaier M, Hoffmann M, Baum A, Lénárt P, Petronczki M, Krssák M, Gürtler U, Garin-Chesa P, Lieb S, Quant J, *et al*: BI 2536, a potent and selective inhibitor of polo-like kinase 1, inhibits tumor growth in vivo. Curr Biol 17: 316-322, 2007.
7. Shin SB, Woo SU and Yim H: Differential cellular effects of Plk1 inhibitors targeting the ATP-binding domain or polo-box domain. J Cell Physiol 230: 3057-3067, 2015.
8. Matthess Y, Raab M, Knecht R, Becker S and Strebhardt K: Sequential Cdk1 and Plk1 phosphorylation of caspase-8 triggers apoptotic cell death during mitosis. Mol Oncol 8: 596-608, 2014.
9. Chen TY, Syu JS, Han TY, Cheng HL, Lu FI and Wang CY: Cell cycle-dependent localization of dynactin subunit p150 glued at centrosome. J Cell Biochem 116: 2049-2060, 2015.
10. Lai PY, Wang CY, Chen WY, Kao YH, Tsai HM, Tachibana T, Chang WC and Chung BC: Steroidogenic factor 1 (NR5A1) resides in centrosomes and maintains genomic stability by controlling centrosome homeostasis. Cell Death Differ 18: 1836-1844, 2011.
11. Wang CY, Kao YH, Lai PY, Chen WY and Chung BC: Steroidogenic factor 1 (NR5A1) maintains centrosome homeostasis in steroidogenic cells by restricting centrosomal DNA-dependent protein kinase activation. Mol Cell Biol 33: 476-484, 2013.
12. Su S, Chhabra G, Singh CK, Ndiaye MA and Ahmad N: PLK1 inhibition-based combination therapies for cancer management. Transl Oncol 16: 101332, 2022.
13. Lian G, Li L, Shi Y, Jing C, Liu J, Guo X, Zhang Q, Dai T, Ye F, Wang Y and Chen M: BI2536, a potent and selective inhibitor of polo-like kinase 1, in combination with cisplatin exerts synergistic effects on gastric cancer cells. Int J Oncol 52: 804-814, 2018.
14. Choi M, Kim W, Cheon MG, Lee CW and Kim JE: Polo-like kinase 1 inhibitor BI2536 causes mitotic catastrophe following activation of the spindle assembly checkpoint in non-small cell lung cancer cells. Cancer Lett 357: 591-601, 2015.

15. Wang CY, Huang EY, Huang SC and Chung BC: DNA-PK/Chk2 induces centrosome amplification during prolonged replication stress. Oncogene 34: 1263-1269, 2015.
16. Chen TY, Huang BM, Tang TK, Chao YY, Xiao XY, Lee PR, Yang LY and Wang CY: Genotoxic stress-activated DNA-PK-p53 cascade and autophagy cooperatively induce ciliogenesis to maintain the DNA damage response. Cell Death Differ 28: 1865-1879, 2021.
17. Wang CY, Tsai HL, Syu JS, Chen TY and Su MT: Primary cilium-regulated EG-VEGF signaling facilitates trophoblast invasion. J Cell Physiol 232: 1467-1477, 2017.
18. Teng YN, Chang HC, Chao YY, Cheng HL, Lien WC and Wang CY: Etoposide triggers cellular senescence by inducing multiple centrosomes and primary cilia in adrenocortical tumor cells. Cells 10: 1466, 2021.
19. Chao YY, Huang BM, Peng IC, Lee PR, Lai YS, Chiu WT, Lin YS, Lin SC, Chang JH, Chen PS, *et al*: ATM- and ATR-induced primary ciliogenesis promotes cisplatin resistance in pancreatic ductal adenocarcinoma. J Cell Physiol 237: 4487-4503, 2022.
20. Wang CY, Chen WY, Lai PY and Chung BC: Distinct functions of steroidogenic factor-1 (NR5A1) in the nucleus and the centrosome. Mol Cell Endocrinol 371: 148-153, 2013.
21. Ferguson RL and Maller JL: Centrosomal localization of cyclin E-Cdk2 is required for initiation of DNA synthesis. Curr Biol 20: 856-860, 2010.
22. Ferguson RL, Pascreau G and Maller JL: The cyclin A centrosomal localization sequence recruits MCM5 and Orc1 to regulate centrosome reduplication. J Cell Sci 123: 2743-2749, 2010.
23. Bailey LJ, Teague R, Kolesar P, Bainbridge LJ, Lindsay HD and Doherty AJ: PLK1 regulates the PrimPol damage tolerance pathway during the cell cycle. Sci Adv 7: eabh1004, 2021.
24. Nakamura K, Kustatscher G, Alabert C, Hödl M, Forne I, Völker-Albert M, Satpathy S, Beyer TE, Mailand N, Choudhary C, *et al*: Proteome dynamics at broken replication forks reveal a distinct ATM-directed repair response suppressing DNA double-strand break ubiquitination. Mol Cell 81: 1084-1099.e6, 2021.
25. Lee M, Daniels MJ and Venkitaraman AR: Phosphorylation of BRCA2 by the Polo-like kinase Plk1 is regulated by DNA damage and mitotic progression. Oncogene 23: 865-872, 2004.
26. Li Z, Li J, Kong Y, Yan S, Ahmad N and Liu X: Plk1 phosphorylation of Mre11 antagonizes the DNA damage response. Cancer Res 77: 3169-3180, 2017.
27. Combes G, Alharbi I, Braga LG and Elowe S: Playing polo during mitosis: PLK1 takes the lead. Oncogene 36: 4819-4827, 2017.
28. Johnson N, Cai D, Kennedy RD, Pathania S, Arora M, Li YC, D'Andrea AD, Parvin JD and Shapiro GI: Cdk1 participates in BRCA1-dependent S phase checkpoint control in response to DNA damage. Mol Cell 35: 327-339, 2009.
29. Ira G, Pellicioli A, Balijja A, Wang X, Fiorani S, Carotenuto W, Liberi G, Bressan D, Wan L, Hollingsworth NM, *et al*: DNA end resection, homologous recombination and DNA damage checkpoint activation require CDK1. Nature 431: 1011-1017, 2004.